Survey on 3D channel modeling : From theory to standardization

Abla Kammoun, Hajer Khanfir, Zwi Altman, Mérouane Debbah, Mohamed Kamoun

Abstract*—Three dimensional beamforming (3D) (also elevation beamforming) is now gaining a growing interest among researchers in wireless communication. The reason can be attributed to its potential to enable a variety of strategies like sector or user specific elevation beamforming and cell-splitting. Since this technique cannot be directly supported by current LTE releases, the 3GPP is now working on defining the required technical specifications. In particular, a large effort is currently made to get accurate 3D channel models that support the elevation dimension. This step is necessary as it will evaluate the potential of 3D beamforming techniques to benefit from the richness of real channels. This work aims at presenting the ongoing 3GPP study item** *"Study on 3D-channel model for Elevation Beamforming and FD-MIMO studies for LTE", and positioning it with respect to previous standardization works.**

I. Introduction

Channel modeling is a fundamental step that allows performance evaluation.While the behavior of the transmitter and the receiver are well understood, the channel, being intrinsically dependent on the surrounding environment, is much more difficult to analyse. This has triggered an increasing activity around channel modeling.

A close look to the evolution of the theory of channel modeling reveals that this field has often been influenced by aspects that were important for the technology available at the time. As a consequence, first channel models used to concentrate on the large scale fading (like Okumara-Hata [1], Lee's model [2]), whereas the small scale fading is reduced to the Doppler effect caused by receiver mobility [3]. Soon after, with the emergence of wideband and multi-antenna technologies, it has been realized that small scale fading should account for the multiple reflections of the emitted signal as well as the spatial correlation between the antenna elements.

In parallel to these theoretical works, there has been a large interest in developing within the framework of wireless standards, reference channel models which serve to define conventional ways to generate channels. For companies, these channel models are of fundamental importance since they allow them to be calibrated to the same channel conditions, and as such to assess system-level and link-level performances of advanced signal processing techniques over real-like channels.

Like their counterparts developed in theoretical works, these channel models have evolved in such a way to address the challenges of wireless communication technologies. The first standardized models were developed in the framework of COST 207 actions [4] which had essentially served to the standardization of GSM. Several actions had been then proposed but it was only with the COST 259 that the spatial structure of the radio channel was taken into account [5]. This was a key step that paved the way towards the modeling of MIMO channels. In fact, influenced by COST actions, 3GPP Spatial Channel Model (SCM) [6], Extended 3GPP [7] and WINNER II [8] have emerged as low complexity alternatives to COST based channel models. While COST actions have continued through COST 273 and COST 2100 to adopt a universal involved concept, SCM and WINNER II introduce several simplifications in order to facilitate system-level simulations. The same simplified approach has been also taken into account in IMT-advanced standardization, strongly inspired by WINNER II and 3GPP2/SCM [9].

To further enhance performance, the actual trend is to exploit the channel's degrees of freedom in the elevation direction. Given that most existing channel models are only two dimensional in that they assume that the wave propagate in the azimuth plane, a large effort in channel modeling has to be made in order to account for the impact of the channel component in the elevation direction. This results in what we refer to as 3D MIMO or full dimension MIMO (FD-MIMO). One way to exploit the additional degree of freedom of 3D channels is to adapt for each user the beam pattern in the vertical direction, thereby improving the signal strength at the receiver and at the same time reducing the interference to other users. Initial implementations of this technology support the potential of this technique for yielding significant gains in real indoor and outdoor deployments [10]. Encouraged by these preliminary results, an extensive research activity on 3D channel modeling is being carried out by both theoretical researchers and industrials. At the time of writing this paper, the TSG-RAN-WG1 of the 3GPP is working on defining next generation channel models in the frame of the study item on elevation beamforming [11]. The outcome of this study will be used for the evaluation of advanced antenna technologies such as 3D beamforming.

Previous surveys on channel modeling and contributions : Channel modeling has been the subject of many surveys. Without tackling multi-antenna modeling, [12] provides a good overview on propagation and large as well as small fading. On the other hand, [13] provides a comprehensive introduction to wireless channel modeling including propagation modeling and statistical description of channels. A detailed overview on propagation modeling with an exclusive summary of mea-

A. Kammoun and M. Debbah are with the Alcatel-Lucent Chair on Flexible Radio, SUPELEC, Gif-sur-Yvette, France (e-mail: {abla.kammoun, merouane.debbah}@supelec.fr). H. Khanfir and Z. Altman are with Orange labs, France (e-mail: {hajer.khanfir,zwi.altman}@orange.com), M. Kamoun is with CEA-LIST, Communicating Systems Laboratory, F-91191 Gif-sur-Yvette, France (e-mail: {mohamed.kamoun@cea.fr})

surement parametrization as well as validation results has been presented in [14]. Very recently, the authors in [15] provide a complete coverage of recent MIMO channel propagation models as well as a description of the most recent signal processing techniques for single-cell/single-user as well as multi-user/multi-cell systems.

Building on these references, our objective in this work is to shed light on the current 3GPP activity around 3D beamforming and FD-MIMO, an aspect that has not been extensively covered to our knowledge. Our recent participation in 3GPP meetings [16], [17] has enabled us to enhance our understanding of the current industrial challenges as well as to deeply comprehend the standards' vision for 3D beamforming. We think that our work contributes to cover new aspects that have not yet been investigated by a research publication. In particular, we adopt a constructive approach that starts from the basics of channel modeling to introduce in a second step standardized channels. In addition to drawing a comparison between the most used models in practice, we report on the progress of the 3GPP activities around the calibration of the future 3D channel.

II. Channel models : From SISO To MIMO channel models

Most existing channel models account for two principal large scale effects which are:

1) Large-scale path loss : Path loss is an average reduction in energy due to the propagation of the electromagnetic wave for a given system configuration. It increases exponentially with distance and carrier frequency. In general, an approximative relation that describes the variation of the path loss with these parameters is determined through measurements. It can also include a loss caused by building penetration for indoor users [6], [8].
2) Large scale fading (shadowing) : It is an average reduction in energy due to the effect of shadowing caused by obstacles, and is mostly modeled as a log-normal distribution [18].

In the sequel, we denote by σ_{SF} and PL the incurred loss caused, respectively, by shadow fading and path loss in dB. We will also focus on the downlink channel between the base station (BS) and the user equipment (UE).

A. SISO Channel Model

Narrowband channel modeling

In case of Narrowband transmissions, the channel can be viewed as a distortion that scales the emitted wave. It is given by:

$$h(t) = 10^{-\frac{\sigma_{SF}+PL}{10}} \exp(\vec{\mathbf{k}} \bullet \vec{\mathbf{r}}_{UE}(t))$$

where $\vec{\mathbf{r}}_{UE}(t)$ denotes the position of the mobile station at time t in the coordinate system corresponding to the UE and $\vec{\mathbf{k}}$ is the wave vector. If the UE is moving with a constant velocity $\vec{\mathbf{v}}_0$ then $\vec{\mathbf{r}}_{UE}(t) = \vec{\mathbf{v}}_0 t + \vec{\mathbf{r}}_{UE,0}$ ($\vec{\mathbf{r}}_{UE,0}$ being the position of the UE at time 0), the resulting channel is equal up to a constant phase to:

$$h(t) = 10^{-\frac{\sigma_{SF}+PL}{10}} \exp(\vec{\mathbf{k}} \bullet \vec{\mathbf{v}}_0 t). \quad (1)$$

Equation (1) reveals that because of the user mobility, the effective frequency is shifted by a $f_D = \frac{\vec{k} \bullet \vec{\mathbf{v}}_0}{c}$ where c is the speed of light. This phenomenon is referred to as the Doppler effect.

Wideband channel modeling

In wideband channel modeling, the propagation delay cannot be neglected compared to the signal period. The received wave is therefore the sum of the contribution stemming from several paths. Each path corresponds to a single or several reflections of the incident wave, [19], [20]. In this case the channel impulse response is obtained by summing the contribution of all possible paths.

$$h(t) = 10^{-\frac{\sigma_{SF}+PL}{10}} \sum_{l=1}^{N_C} \alpha_l(t) \delta(t - \tau_l). \quad (2)$$

where $\alpha_l(t)$ represents the additional attenuation corresponding to the l-th path.

B. MIMO channel Models

As we have noted above, SISO channel models are fully characterized by the statistics of the delays and powers of each path. However, this information becomes highly insufficient to capture the richness of MIMO channels.

1) Double Directional MIMO Channel: To describe MIMO channels, it can be useful to distinguish between the radio channel and the propagation channel which only depends on the environment and excludes as such the effect of antenna responses. This propagation channel is referred to as double-directional channel model, [21], [22]. It does not depend on the number of antennas at the receiver or the transmitter. Actually, it is a scalar or a 2×2 matrix if dual-polarization is considered.

In addition to the delays, the double directional model depends on the directions of departure and the directions of arrival. The double directional impulse function corresponding to the ℓ-th multipath component (MPC) is thus given by:

$$h_\ell(t, \tau, \Omega, \Psi) = \alpha_\ell \delta(\tau - \tau_\ell) \delta(\Omega - \Omega_l) \delta(\Psi - \Psi_l) \exp(j\vec{\mathbf{k}}_{\ell,r} \bullet \vec{\mathbf{r}})$$

where τ is the delay variable and Ω, Ψ stand for the spatial angles respectively at the transmitter and the receiver, i.e., $\Omega = (\phi, \theta)$ and $\Psi = (\varphi, \vartheta)$ where ϕ and φ are the departure and arrival azimuth angles whereas θ and ϑ are the departure and arrival elevation angles (See Fig. 4).

Besides, α_l is the complex amplitude of the path l whereas $\vec{\mathbf{r}}$ is the position of the receiver at time t and $\vec{\mathbf{k}}_{\ell,r}$ is the wave vector corresponding to the received wave vector of the ℓ th path.

The double directional impulse response is the sum of the N_C MPCs and is given by:

$$h(t, \tau, \Omega, \Psi) = \sum_{l=1}^{N_C} \alpha_\ell \delta(\tau - \tau_\ell) \delta(\Omega - \Omega_l) \delta(\Psi - \Psi_l) \exp(j\vec{\mathbf{k}}_l \bullet \vec{\mathbf{r}}) \quad (3)$$

If polarization is taken into account, α_ℓ and thus $h(t, \tau, \Omega, \Psi)$ are 2×2 matrices which describe the coupling between vertical and horizontal polarizations [23] :

$$\mathbf{h}(t, \tau, \Omega, \Psi) = \begin{bmatrix} h^{VV}(t, \tau, \Omega, \Psi) & h^{VH}(t, \tau, \Omega, \Psi) \\ h^{HV}(t, \tau, \Omega, \Psi) & h^{HH}(t, \tau, \Omega, \Psi). \end{bmatrix}$$

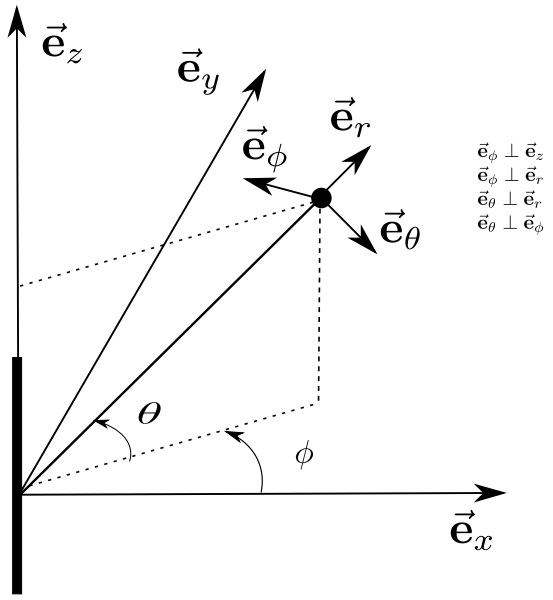

Fig. 1. A vertically polarized antenna element

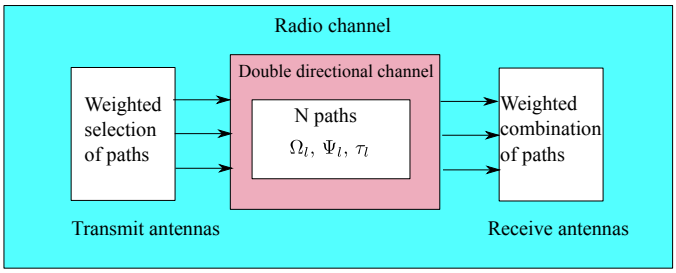

Fig. 2. The radio channel

In other words, the elements $h^{VV}(t,\tau,\Omega,\Psi)$ and $h^{VH}(t,\tau,\Omega,\Psi)$ represent up to a scalar what would be obtained by a receiver in the vertical and horizontal directions if the transmitted wave is vertically polarized. In the same way, the elements $h^{HH}(t,\tau,\Omega,\Psi)$ and $h^{HV}(t,\tau,\Omega,\Psi)$ represent up to scalar what would be received in the horizontal and vertical polarizations if the transmitted wave is horizontally polarized. For the reader convenience, we recall that If $(\vec{\mathbf{e}}_r,\vec{\mathbf{e}}_\theta,\vec{\mathbf{e}}_\phi)$ is the spherical coordinate system associated to the vertical to the ground $\vec{\mathbf{e}}_z$, vertical polarization refers to the polarization along $\vec{\mathbf{e}}_\theta$ whereas horizontal polarization refers to the polarization along $\vec{\mathbf{e}}_\phi$. In particular, a vertically oriented antenna elements delivers an electric field which is along $\vec{\mathbf{e}}_\theta$ (See Fig. 1).

2) Radio channel: The radio channel is obtained by incorporating the effect of the antennas. This can be modeled at the reception or the transmission side as a coherent sum over all directions, (see Fig.2). Let N_T and N_R denote the number of the transmitting and receiving antennas. The radio channel is a $N_R \times N_T$ matrix given by:

$$\mathbf{H}(t,\tau) = \int \vec{\mathbf{g}}_r(\Psi)^{\mathrm{T}} h(t,\tau,\Omega,\Psi)\vec{\mathbf{g}}_T(\Omega)\vec{\mathbf{a}}_R(\Psi)\left(\vec{\mathbf{a}}_T(\Omega)\right)^{\mathrm{T}} d\Omega d\Psi$$

where :

- $\vec{\mathbf{g}}_r$ and $\vec{\mathbf{g}}_T$ are the patterns of the receiving and transmitting antennas. When polarization is considered, $\vec{\mathbf{g}}_r(\Psi)$ and $\vec{\mathbf{g}}_T$ are 2×1 vectors whose entries represent the vertical and horizontal field patterns.
- Vectors $\vec{\mathbf{a}}_R(\Psi)$ and $\vec{\mathbf{a}}_T(\Omega)$ are the array responses of the transmitting and receiving antennas whose entries are given by:

$$\left[\vec{\mathbf{a}}_R(\Psi)\right]_i = \exp\left(\jmath\vec{\mathbf{k}}_{R,\Psi}\bullet\vec{\mathbf{x}}_{R,i}\right)$$
$$\left[\vec{\mathbf{a}}_R(\Psi)\right]_i = \exp\left(\jmath\vec{\mathbf{k}}_{T,\Psi}\bullet\vec{\mathbf{x}}_{T,i}\right)$$

where $\vec{\mathbf{x}}_{R,i}$ is the location vector of the ith receiving antenna whereas $\vec{\mathbf{x}}_{T,i}$ is that of the ith transmitting antenna. These location vectors are computed with respect to the global cartesian coordinate system $(\vec{\mathbf{e}}_x,\vec{\mathbf{e}}_y,\vec{\mathbf{e}}_z)$, (See Fig. 1). Substituting $h(t,\tau,\Omega,\Psi)$ by its expression, the radio channel writes as:

$$\mathbf{H}(t,\tau) = \sum_{\ell=1}^{N_C} \delta(\tau-\tau_\ell)\vec{\mathbf{g}}_r(\Psi_\ell)^{\mathrm{T}}\boldsymbol{\alpha}_l\vec{\mathbf{g}}_T(\Omega_\ell)\vec{\mathbf{a}}_R(\Psi_\ell)\left(\vec{\mathbf{a}}_T(\Omega_\ell)\right)^{\mathrm{T}} \tag{4}$$

Equation (4) is generic in that it encompasses several kind of channel models. In particular, if the spatial angle Ω or Ψ are defined using only the azimuth, the channel is said to be two-dimensional (2D), whereas (3D) channels are obtained by accounting for both elevation and azimuth angles.

III. Standardized channel models

A. Generation of the channel in system level approach based standards

Building on the theoretical framework of channel modeling, standards based on a system level approach rely on the same findings described by (4). In a similar way as above, the channel is composed of many propagation paths with different time delays, referred to as *clusters*. Each cluster is characterized by three quantities : the delay τ_n, the spatial angle of departure $\Omega_n = (\theta_n,\phi_n)$ and the spatial angle of arrival $\Psi_n = (\vartheta_n,\varphi_n)$. However, the standardized channel models differ from those described in the previous section in that it is assumed that each cluster gives rise to M_n unresolvable paths which have the same delay as the original cluster. Moreover, each sub-path is characterized by its spatial angles $\Omega_{n,m} = (\theta_{n,m},\phi_{n,m})$ and $\Psi_{n,m} = (\vartheta_{n,m},\varphi_{n,m})$ where

$$\theta_{n,m} = \theta_n + c_\theta\alpha_m, \qquad \phi_{n,m} = \phi_n + c_\phi\alpha_m$$
$$\vartheta_{n,m} = \vartheta_n + c_\vartheta\alpha_m, \qquad \varphi_{n,m} = \varphi_n + c_\varphi\alpha_m$$

and $\alpha_m, m = 1,\cdots,M_n$ is a set of symmetric fixed values and c_ϕ, c_θ, c_φ and c_φ controls the spread inside the cluster n, (See Fig. 4).

The channel response corresponding to the n-th path is thus given by:

$$\mathbf{H}_n(t) = \sqrt{10^{-(PL+\sigma_{SF})/10}}\sum_{m=1}^{M_n}\sqrt{P_{n,m}}\vec{\mathbf{g}}_R(\varphi_{n,m},\vartheta_{n,m})^{\mathrm{T}}\boldsymbol{\alpha}_{n,m}$$
$$\times\,\vec{\mathbf{g}}_T(\phi_{n,m},\theta_{n,m})\vec{\mathbf{a}}_R\left(\varphi_{n,m},\vartheta_{n,m}\right)$$
$$\times\,\vec{\mathbf{a}}_T(\phi_{n,m},\theta_{n,m})^{\mathrm{T}}\exp\left(\jmath\vec{\mathbf{k}}_{r,n,m}\bullet\vec{\mathbf{v}}t\right)$$

where $\vec{\mathbf{k}}_{r,n,m}$ is the wave vector corresponding to the m-th subpath, $P_{n,m}$ is the energy of the m-th subpath and

$$\boldsymbol{\alpha}_{n,m} = \begin{bmatrix} \exp\left(\jmath\Phi_{n,m}^{VV}\right) & \sqrt{\kappa_{n,m}}\exp\left(\jmath\Phi_{n,m}^{VH}\right) \\ \sqrt{\kappa_{n,m}}\exp\left(\jmath\Phi_{n,m}^{HV}\right) & \exp\left(\jmath\Phi_{n,m}^{HH}\right) \end{bmatrix},$$

$\kappa_{n,m}$ being the cross-polarization ratio and $\Phi_{n,m}^{HH}$, $\Phi_{n,m}^{HV}$, $\Phi_{n,m}^{VH}$, and $\Phi_{n,m}^{VV}$ being random phases. If the UE is on Line of sight (LOS) with respect to the cell, it is assumed that the first cluster contains the line-of-sight (LOS) contribution of the channel. In this case, the channel response is given by (5), where $\boldsymbol{\alpha_{LOS}} = \begin{bmatrix} \exp\left(\jmath\Phi_{LOS}^{VV}\right) & 0 \\ 0 & \exp\left(\jmath\Phi_{LOS}^{HH}\right) \end{bmatrix}$, $\vec{\mathbf{k}}_{r,LOS}$ is the wave vector along the line-of-sight direction and K is the rice factor [1].

Most standardized channels like SCM, SCME, WINNER and ITU are based on the model described by (5). It is thus no surprise that these models share almost the same procedure for generating the channel. Unlike the COST family of channel models, WINNER, ITU, SCM and SCME follow a system level approach, in which without being physically positioned, clusters are described through statistical parameters, known as *large scale parameters*. These latter are random correlated variables drawn from given distributions, and are specific for each user. They serve to generate powers, delays and angles of each path, which are often referred to as *small scale parameters* in that they describe the channel at a microscopic level.

The generation of the channel in system level approach based standards follows three main steps:

1) Choice of the scenario and dropping of the UEs. For each UE, general parameters (position, pathloss, Large scale parameters, Propagation Mode, ...) are then set.
2) Generation of the small scale parameters is performed based on the obtained large scale parameters in step 1).
3) With the small scale parameters on hand, the channel is computed using (5).

While system level approach based channels follow the same philosophy, they differentiate in the way the slow fading and the small scale parameters are generated. The reason is that these channels support different frequencies and are tuned using different measurement campaigns. Hereafter, we illustrate the main principal differences between these models.

- Number of scenarios : SCM was dedicated originally to outdoor channel models. It defines three scenarios which are urban micro, urban macro and suburban macro. SCME keeps the same number of scenarios but WINNER II and ITU extends the channel to more scenarios (5 channels for ITU and 17 scenarios for WINNER II).
- Frequency range: Channel models depend on the frequency through the pathloss. While the SCM channel model is adjusted for frequencies of 1.9GHz, SCME, ITU and WINNER II, support a range of frequency of 2-6 Ghz.
- Bandwidth and number of clusters : The SCM channel was targeted to up to 5MHz RF bandwidth. Thus, only 6 clusters with different delays were found to be sufficient. SCME which is an extension of SCM to bandwidths up to 100Mhz modifies the number of effective clusters by subdividing each cluster to 3 or 4 sub-clusters with different delays, while keeping the same number of multi-path components. In WINNER II and ITU, the number of clusters is increased and depends on the scenario, whereas the two strongest clusters are subdivided using almost the same technique proposed in SCME.
- Propagation mode : In SCM, the LOS propagation mode is defined only in the ubran micro scenario, whereas only the NLOS is considered for the other scenarios. On the other hand, WINNER II defines for some specific scenarios a third propagation mode namely the obstructed-line-of-sight (OLOS) to describe the situation where the LOS direction is obstructed but still remains dominant. Moreover, it usually supports both propagation mode (LOS and NLOS) except for some scenarios where only the LOS or the NLOS is allowed. On the contrary, ITU always supports LOS and NLOS propagation modes for its five scenarios. It also defines a third propagation mode in the UMI scenario namely the outdoor to indoor propagation mode which serves to describe the situation where the UE is inside a building. This is to be compared with WINNER II which defines a fully-fledged scenario [8] (scenario B4) to account for the outdoor to indoor link.
- 2D vs 3D channel models : Almost all the system level approach based standards are 2 dimensional. This implies that all the waves are in the azimuth plane (plane parallel to the ground). The unique 3D standard based on the system level approach is WINNER+ [24] which is an extension of WINNER II to the three dimensional case. The difference between three and two dimensional models is illustrated in Fig. 4 and Fig. 3.
- Large scale parameters : Large scale parameters describe the channel at a macroscopic level in that they control the distributions of small scale parameters. They are random correlated variables that are generated for each link between a UE and a site (See (III-D)). In 3GPP, three large scale parameters are considered which are the delay spread, the departure azimuth angular spread and the shadow fading. To these large scale parameters, WINNER II and ITU add the arrival azimuth spreads and the rician factor, thereby increasing the number of large scale parameters to 5. By considering elevation, WINNER+ accounts for 7 large scale parameters which include the departure and arrival elevation spreads.

B. Antenna configuration

To make it easier for the reader to understand the use of the 3D beamforming technique in practice, we shall introduce in this section the antenna configuration that is being proposed in current standardization works. In LTE, the radio resource is organized on the basis of antenna ports. Each antenna port is mapped to a group of physical antenna elements which carry the same signal. As a consequence, each antenna port

[1]Note that (5) encompasses the non-line-of-sight(NLOS) case by taking $K = 0$.

$$\mathbf{H}_n(t) = \sqrt{10^{-\frac{PL+\sigma_{SF}}{10}}} \left(\sqrt{\frac{1}{K+1}} \sum_{m=1}^{M_n} \sqrt{P_{n,m}} \vec{\mathbf{g}}_R \left(\varphi_{n,m}, \vartheta_{n,m}\right)^{\mathrm{T}} \boldsymbol{\alpha}_{n,m} \vec{\mathbf{g}}_T \left(\phi_{n,m}, \theta_{n,m}\right) \vec{\mathbf{a}}_R \left(\varphi_{n,m}, \vartheta_{n,m}\right) \vec{\mathbf{a}}_T \left(\phi_{n,m}, \theta_{n,m}\right)^{\mathrm{T}} \right.$$
$$\left. \times \exp\left(j\vec{\mathbf{k}}_{r,n,m} \cdot \vec{\mathbf{v}} t\right) + \delta(n-1) \sqrt{\frac{K}{K+1}} \vec{\mathbf{g}}_R \left(\varphi_{LOS}, \vartheta_{LOS}\right)^{\mathrm{T}} \boldsymbol{\alpha}_{LOS} \vec{\mathbf{g}}_T \left(\phi_{LOS}, \theta_{LOS}\right) \exp\left(j\vec{\mathbf{k}}_{r,LOS} \cdot \vec{\mathbf{v}} t\right) \right) \quad (5)$$

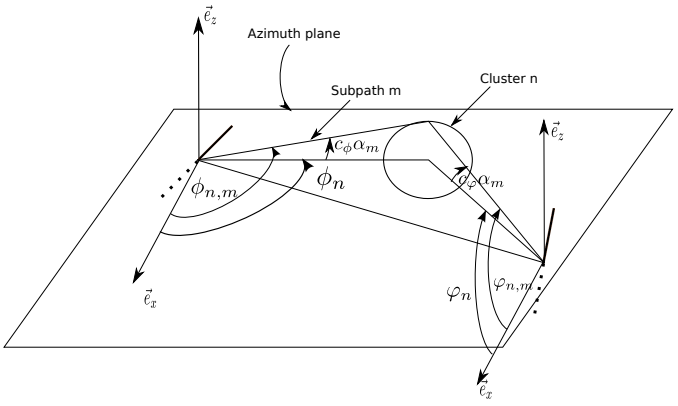

Fig. 3. 2D channel model

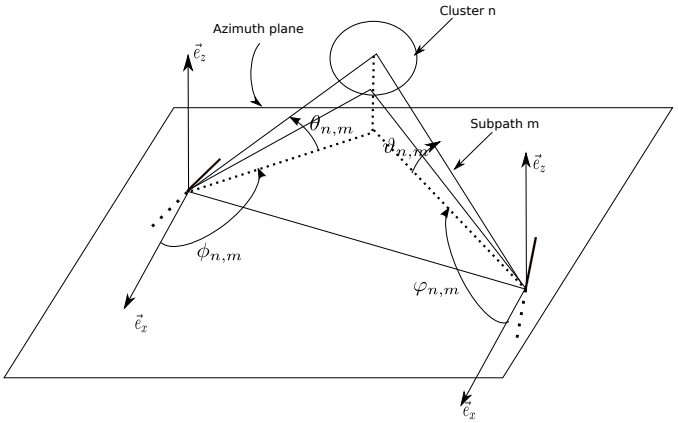

Fig. 4. 3D channel model

is viewed as a single antenna at the receiver side. In LTE, these antenna ports are used to support different transmission modes [25]. For instance, in mode 7, antenna port 5 is used to transmit only one stream, a configuration which is often referred to as single layer transmission. This antenna port is mapped to more than one antenna element. The signal is fed to each of the antenna elements with a corresponding weight in order to focus the wavefront in the direction of the UE. Since the weights are not extracted from a code-book, this technique is called non-codebook based precoding (See fig. 5). At the receiver side, each antenna port appears as a single antenna, because its elements carry the same signal. It is thus no surprise that we are interested rather on the channel between the transmitting antenna port and the receiver side. For that, in (5) it is the antenna port pattern that should be used and not the antenna element pattern.

In theory, the antenna port pattern depends on the number of antenna elements, their patterns, as well as their relative

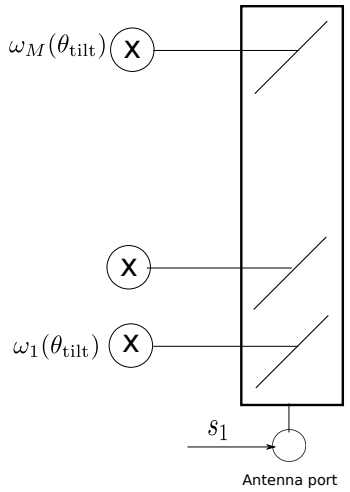

Fig. 5. Antenna port

positions and their corresponding weights. To enable an abstraction of the role played by the antenna elements to perform the downtilt, ITU channel model approximates the pattern of each antenna port by a narrow beam in the elevation plane with $\theta_{3\text{dB}} = 15^\circ$. In fact the combined pattern considered in ITU is given by:

$$A_P(\phi, \theta) = G_{P,\max} - \min\left\{-\left(A_H(\phi) + A_V(\theta)\right), A_m\right\},$$
$$A_m = 20dB, G_{P,\max} = 17dBi$$

where

$$A_H(\phi) = -\min\left[12\left(\frac{\phi}{\phi_{3\text{dB}}}\right)^2, A_m\right]$$
$$\phi_{3\text{dB}} = 70^\circ$$

and

$$A_V(\theta) = -\min\left[12\left(\frac{\theta - \theta_{\text{tilt}}}{\theta_{3\text{dB}}}\right)^2, A_m\right]$$
$$\theta_{3\text{dB}} = 15^\circ$$

where θ_{tilt} is the electrical tilt angle. This approach despite its simplicity poses a problem when dual-polarized channels are used. In fact, while standards provide the expression of the global pattern at each antenna port, they do not show how one can deduce the horizontal and vertical field patterns. To circumvent this difficulty, the document 3GPP 36.814 [26, section A.2.1.6.1, page 79] proposes to model the polarization *as angle independent in both azimuth and elevation*. Recall that in the case of dual-polarized channels, each antenna port is composed of cross-polarized antenna elements that are slanted

in the plane perpendicular to the boresight (direction of the maximum gain) by a slant angle α.

If $A(\phi,\theta)$ denotes the global pattern of the transmitting antenna port when each element is vertically polarized, then after slanting each antenna element by a slant angle α in the plane perpendicular to the boresight, the global pattern along horizontal and vertical polarizations is approximated according to the document 3GPP 36.814 by:

$$\mathbf{g}_T(\phi,\theta) = \left[\sqrt{A(\phi,\theta)_{\text{lin}}}\cos\alpha, \sqrt{A(\phi,\theta)_{\text{lin}}}\sin\alpha\right]$$

Obviously, such an approximation does not hold in practice. It is only valid at the boresight direction. To determine the right decomposition of the antenna pattern on the vertical and horizontal polarizations, one has to know exactly the exact structure of the antenna port, i.e, the exact number of antenna elements, as well as their relative positions. This information was missing, because the adopted strategy was to rely on the channel with each transmitting antenna port rather than that with each transmitting antenna element, [27].

C. 3D Beamforming

At the time of the writing of this paper, the TSG-RAN-WG1 is investigating the use of 3D beamforming for next generation systems. In order to enable optimization of this technique, the channel between antenna elements rather than that between antenna ports is considered. It is also assumed that antennas are arranged in a 2D array where each column contains M antenna elements. There are exactly K antenna elements per antenna port with a pattern A_E given by:

$$A_E(\phi,\theta) = G_{E,\max} - \min\left\{-\left(A_H(\phi) + A_V(\theta)\right), A_m\right\},$$
$$A_m = 30dB, G_{E,\max} = 8dBi$$

where

$$A_H(\phi) = -\min\left[12\left(\frac{\phi}{\phi_{3\text{dB}}}\right)^2, A_m\right]$$
$$\phi_{3\text{dB}} = 65\text{degrees}$$

and

$$A_V(\theta) = -\min\left[12\left(\frac{\theta-\theta_{\text{tilt}}}{\theta_{3\text{dB}}}\right)^2, SLAV\right]$$
$$SLAV = 30, \theta_{3\text{dB}} = 65\text{degrees}$$

Two cases are considered by the 3GPP group TSG-RAN-WG1, either choosing $K = 1$ in which case the number of antenna ports per column will be equal to M or setting $K = M$, in which case, each column will correspond to one port with the same polarization (see Fig. 6 and Fig. 7). Note that, if cross-polarized elements were used, each column would correspond to two ports, (one port per polarization). The channel with a given antenna port is a weighted sum of channels with the K antenna elements inside it. More formally, the channel between the uth receiving antenna and the sth antenna port corresponding to the nth path is given by:

$$\left[\overline{\mathbf{H}}_n\right]_{s,u} = \sum_{k\in \text{ port } s} \omega_k \left[\mathbf{H}_n\right]_{k,u}$$

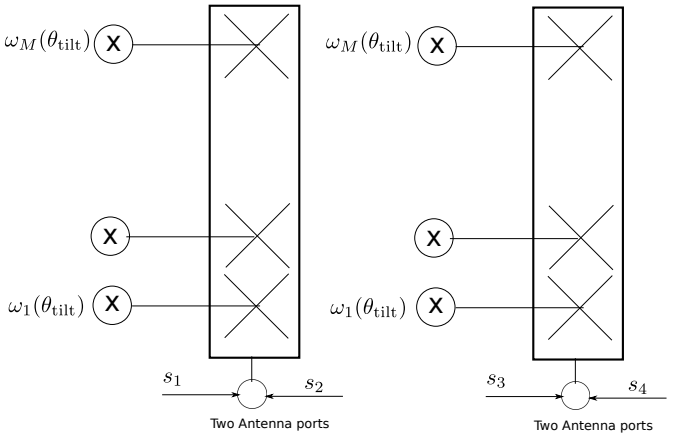

Fig. 6. $K = M$

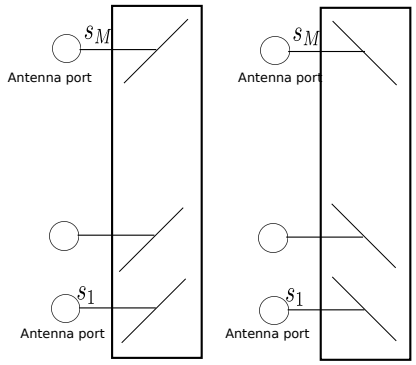

Fig. 7. $K = 1$

where the sum above is performed over all antenna elements in port s and $\mathbf{H}_n$ is computed by using in (5) the field patterns of one antenna element. This field pattern could be easily retrieved by determining the coordinate transformation between the local and the global spherical coordinate system, [28] [2].

The objective of the channel representation based on the antenna elements is two folds: First it enables to take into account the pattern of side lobes, an effect which has been discarded by the channel representation in ITU [9] and 3GPP 36.814 [26]. And second, it allows more flexibility, the channel being linearly dependent on the weights ω_k. We can also add a third advantage which is the possibility of providing accurate expressions for the vertical and horizontal field patterns. This has been the subject of our contribution [28] which was prepared for meeting RAN1#74 but only off-line submitted. Two meetings later, our polarization model was proposed by NSN, Nokia [29], Qualcomm [30] and Fraunhofer [31].

D. System level simulations

The new channel model that is now being prepared by 3GPP will serve to perform system level simulations. A network of 19 sites is considered, where each site is composed of tri-sector base stations (See Fig. 8). Each base station is equipped with

[2]The local spherical coordinate system is defined by the antenna axis $\vec{\mathbf{e}}_{za}$, i.e, $\vec{\mathbf{e}}_\phi = \frac{\vec{\mathbf{e}}_r \times \vec{\mathbf{e}}_{za}}{\|\vec{\mathbf{e}}_r \times \vec{\mathbf{e}}_{za}\|}$ and $\vec{\mathbf{e}}_\theta = \vec{\mathbf{e}}_\phi \times \vec{\mathbf{e}}_r$, where $\times$ being the cross-product.

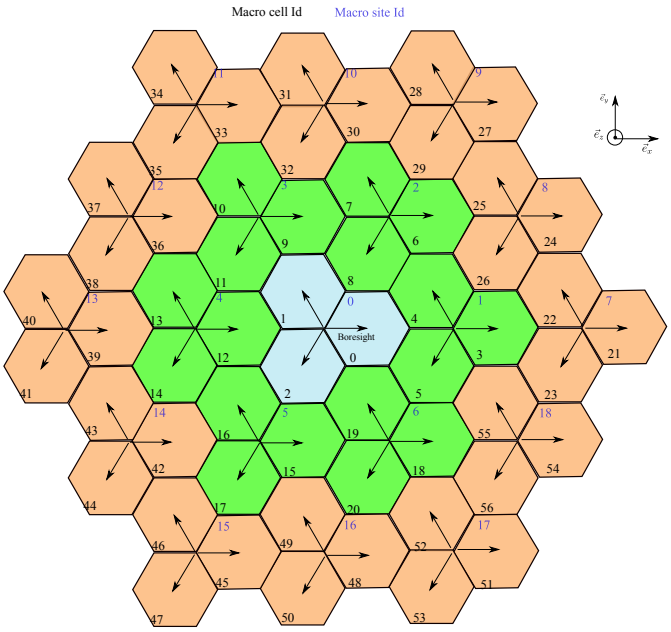

Fig. 8. Network Layout

a 2D antenna array structure composed of M rows and N columns. The TSG-RAN-WG1 is considering the scenario of Urban-Micro (UMi) and Urban-Macro (UMa). Measurement campaigns are currently being performed in order to tune the large scale parameters, as well as, the slow fading. An important progress has been made. An agreement has been already reached for the slow fading parameters. Also, the tuning of the large scale parameters is at a final stage. The document [32] contains all the decisions as well as some of the few remaining issues.

For the reader convenience, we summarize in the next section the new elements which make the difference with previous channel models.

1) New elements:

a) 3D UE dropping : In previous standardized channel models, all the UE are assumed to have a height of $1.5m$. With such UE dropping, the elevation of the LOS direction depends on the distance between the BS and the UE : the closest is the UE to the BS, the largest is the elevation corresponding to the LOS direction. As such, users undergoing similar slow fading channel conditions will show almost the same elevation in the LOS direction, making it difficult to perform vertical separation. In light of this consideration, the TSG-RAN WG1 is working on 3D UE Dropping. With this new dropping, each user is outdoors in only 20% of the cases, in which situation its height is set to $1.5m$. If it is indoors, then it is inside a building of x floors where x is a random variable uniformly chosen from the set $\{4, 5, 6, 7, 8\}$. Finally, the UE floor n_{fl} is uniform-randomly selected from the set $\{1, \cdots, x\}$ while the UE height is given by $h_{UE} = 3(n_{fl} - 1) + 1.5$.

b) Outdoor to Indoor users for UMa and UMi : In the ITU channel, the outdoor-to indoor connection is a propagation mode specific to the Urban-Microcell scenario which was proposed to support UEs inside buildings. The 3GPP new channel model will extend this propagation mode to the UMa since this scenario will consider also indoor users.

c) High rise scenario : High rise scenario is an optional scenario proposed by CMCC [33] in meeting RAN1$\#74$ to describe the channel of UEs in very high floors (above 20). To cover these users, a possible way is to deploy indoor distributed antenna systems, an alternative which has been already deployed in high office buildings. Unfortunately, this solution cannot be always applied for high residence buildings. In this case, the use of uptilt beams can be proposed.

d) Antenna height correction factor for the path loss: It is well known that, in addition to the frequency and the distance with the UE, the path loss depends also on the heights of transmitting and receiving antennas [34]. A correction factor should be thus introduced in order to account for these dependencies. Based on measurements, the TSG-RAN-WG1 modifies the pathloss expressions of the ITU channel model in order to account for the impact of the UE height in NLOS conditions.

e) Distance dependent large scale parameters : Very recently, based on measurements, NSN, Nokia proposes to model the elevation spreads as log-normal random variables whose parameters depend on the 2D distance for UMa scenarios and on both the 2D distance and the mobile height for UMi scenarios, [35]. This model has just been approved in meeting RAN1$\#75$.

f) UE Attachment Policy : In system level simulators, the determination of the serving cell for each UE is based on a metric known as RSRP (Reference Signal Received Power). Currently, the computation of the RSRP is based solely on the slow fading parameters (Pathloss + shadow fading). More details about the computation of the RSRP in this case is given in section 2.a) dealing with phase 1 calibration. For phase 2 and phase 3 calibrations, it has just been agreed in meeting RAN1$\#75$ to account also for fast fading [36]. This method should be more accurate, since unlike the azimuth angles, the elevation angles are modeled as random variables whose mean is shifted by a constant angle from the LOS direction.

2) Calibration: Companies and organizations involved in channel standardization conduct measurements campaigns in order to tune the channel system parameters. Once an agreement is reached, companies implement the channel in their own simulation tools, which are not publicly available. Although being based on the same channel model, companies come in general to different system performances. The reason can be attributed to either a mismatch on scheduling algorithms which are not standardized, or to some errors in the code, a problem which is likely to often occur given the high complexity of the simulation procedure. To exclude the second reason, channel calibration is often performed. For calibrations that do not consider a transmission scheme, all companies have to get exactly the same results. The TSG-RAN WG1 considers three calibration phases. We present hereafter these calibrations as well as the obtained so far results.

a) Phase 1 Calibration : Phase 1 calibration relies only on the slow fading parameters. The objective of this phase is to compute the empirical cumulative distribution function (CDF) of two metrics referred to as coupling gain and geometry factor. The coupling gain measures the difference between the received signal and the transmitted signal along the line-of sight direction. On the other hand, the geometry factor measures the signal to interference ratio with respect to the serving cell. At the time of the writing of the paper, TSG-RAN WG1 has just finished the calibration phase 1. We will present in this section our results which comply with those obtained by companies. But, before that, we detail hereafter for the reader convenience the procedure that has been followed to achieve the phase 1 calibration. After performing UE dropping, this phase consists in computing for each UE m and site k the following quantities :

- The LOS direction characterized by a spatial angle $\Omega_{k,m} = (\phi_{LOS,k,m}, \theta_{LOS,k,m})$ and $\Psi_k = (\varphi_{LOS,k,m}, \vartheta_{LOS,k,m})$ with respect to the k-th cell,
- For each cell i in the site ($i = 1, 2, 3$), compute the antenna gain at the transmitter and the receiver $G_T(\phi_{LOS,k,m,i}, \theta_{LOS,k,m,i})$ and $G_R(\varphi_{LOS,k,m,i}, \vartheta_{LOS,k,m,i})$ in dB,
- Compute the pathLoss $PL_{k,m}$ and shadow-fading $\sigma_{SF_{k,m}}$ between the UE and cell k,
- Define for the user, the $RSRP_{k,m,i}$ (Reference Signal Received Power)

$$\begin{aligned} RSRP_{k,m,i} = P_{TX} &+ G_T(\phi_{LOS,k,m,i}, \theta_{LOS,k,m,i}) \\ &+ G_R(\phi_{LOS,k,m,i}, \theta_{LOS,k,m,i}) \\ &- PL_{k,m}(dB) - \sigma_{SF,k,m}(dB) \end{aligned}$$

  where P_{TX} is the transmitted power in dB.
- Determine the index $\overline{k}_m$ and $\overline{i}_m$ of the best serving cell which maximizes the RSRP.
- The coupling gain for the UE m is defined as:

$$CL_m = RSRP_{\overline{k}_m, \overline{i}_m} - P_{TX}$$

- The geometry factor for the UE m is given by:

$$GF = RSRP_{\overline{k}_m, \overline{i}_m, m} - \sum_{(k,i) \neq (\overline{k}_m, \overline{i}_m)} RSRP_{k,i,m}$$

We present in Fig. 9 and Fig. 10, the obtained results of the geometry factor for the UMa scenario when the vertical spacing is equal to 0.5λ and 0.8λ. These results comply with those obtained by industrial contributions. Note that for $d_v = 0.5\lambda$ the downtilt of 12 degree achieves the best performance. This is to be compared to the case where $d_v = 0.8\lambda$ for which the best dowtilt value is given by 9 degree. In this case, the reduction of inter-cell interference for high downtilt angles (12 degree) cannot compensate the degradation in coupling gain which is amplified by the fact that the beam is narrower.

b) Phase 2 and Phase 3 Calibrations : Phase 2 and Phase 3 calibrations are now being conducted by the TSG-RAN-WG1. As we mentioned above, for phase 2 and 3 calibrations, the computation of the RSRP takes into account the fast fading. For each m UE and site k, large scale parameters describing the distribution of the azimuth and elevation angles are generated. With these large scale parameters on hand, small scale parameters including azimuth and elevation angles, powers and delays are generated for each UE and cells. Note that the links between a UE and cells in the same site share the same large scale parameters but different small scale parameters. Unlike phase 1 calibration, the RSRP for all the link is computed based on the fast fading in addition to the slow fading. The UE is then associated to the base station which delivers the highest RSRP.

For phase 2 calibration, companies should give CDF curves for the azimuth and elevation angular spreads as well as for the delay spread. To calibrate the channel generation procedure, CDF of the first and second largest eigenvalues of the channel should also be presented [36].

Finally for phase 3 calibration, a transmission scheme will be considered, and the system level performances will be expressed in terms cell coverage, cell edge throughput and spectrum efficiency, [37].

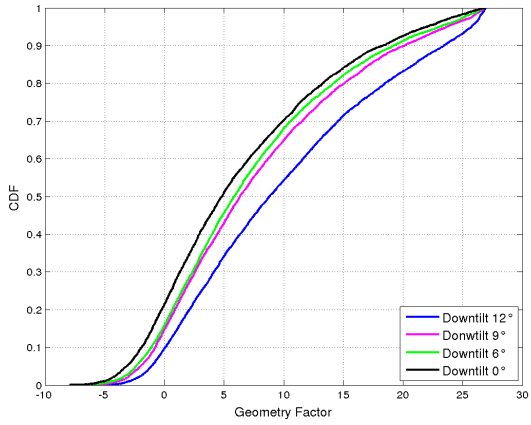

Fig. 9. Geometry factor for $d_v = 0.5\lambda$

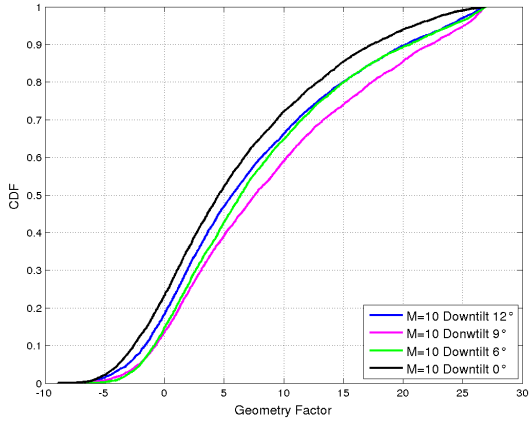

Fig. 10. Geometry factor for $d_v = 0.8\lambda$

IV. Conclusion

Channel modeling is sparking increasing interest from both academia and industry. A number of different approaches in standards and theory have arisen. Nevertheless, few works have considered to establish a common thread between them. This has been in particular the objective of our work. After a brief overview on the theoretical basics of channel modeling, we have presented some of the most used standardized channel models, with a special focus on their different and common properties. A close inspection of these models reveals that they have evolved towards a higher complexity as they should satisfy more stringent requirements. At the moment, a large effort is being made within the 3GPP TSG-RAN-WG1 group to produce accurate 3D channel models, thereby paving the way towards 3D beamforming techniques. In this line, we have provided in this paper a brief overview on the calibrations that are being carried out by the 3GPP, as well as some initial results concerning phase 1 calibration.

References

[1] M. Hata, "Empirical Formulas for Propagation Loss in Land Mobile Radio Service," *IEEE Trans. Veh. Technol.*, vol. 29, no. 3, pp. 317–325, Aug. 1980.

[2] W. C. Y. Lee, *Mobile Communications Engineering*, McGrawHill, New York, 1982.

[3] W. C. Jakes, "A Comparison of Specific Space Diversity Techniques for Reduction of Fast Fading in UHF Mobile Radio Systems," *IEEE Trans. Veh. Technol.*, vol. 20, no. 4, pp. 81–91, Nov. 1971.

[4] M. Failli, "Digital Land Mobile Communications COST 207 Final Report," 1989.

[5] L. M. Correia, *Wireless Flexible Personalized Communications COST 259:European Co-operation in Mobile Radio Research* , John Wiley & Sons, New York, 2001.

[6] "3GPP TR 25.996 V6.1.0 (2003-09) Technical Report," 2003.

[7] D. S. Baum, J. Hansen, and J. Salo, "An Interim Channel Model for Beyond 3G Systems : Extending the 3GPP Spatial Channel Model (SCM)," in *Proc. IEEE Vehicular Technology Conference*, May 2005, vol. 5, pp. 3132–3136.

[8] P. Kyösti, "WINNER II Channel Models, DR1.1.2," 2007.

[9] Report ITU-R M.2135, "Guidelines for evaluation of radio interface technologies for imt-advanced," 2008.

[10] J. Koppenborg, H. Halbauer, S. Saur, and C. Hoek, "3D Beamforming Trials with an Active Antenna Array," in *ITG Workshop on Smart Antennas*, 2012.

[11] R1-122034, "Study on 3D channel Model for elevation Beamforming and FD-MIMO studies for LTE," *3GPP TSG RAN Plenary # 58*, Dec. 2012.

[12] T. Rappaport, *Wireless Communications, Principles and Practice*, Prentice-Hall, Englewood Cliffs, NJ, USA, 1996.

[13] A. F. Molish, *Wireless Communications*, Wiley IEEE Press, New York,NY, USA, 2005.

[14] L. Correia, *Mobile Broadband Multimedia Networks*, John Wiley & Sons, New York, NY, USA, 2006.

[15] B. Clerckx and C. Oestges, *MIMO Wireless Networks : Channels, Techniques and Standards for Multi-antenna, Multi-User and Multi-Cell Systems*, Academic Press (Elsevier), Oxford, UK, Jan. 2013.

[16] R1-133719, "Initial Results for 3D channel Model UMa Calibration Case 1, Orange," *3GPP TSG RAN1 Meeting #74*, Aug. 2013.

[17] R1-133720, "Initial Results for 3D channel Model UMa Calibration Case 3, Orange," *3GPP TSG RAN1 Meeting #74*, Aug. 2013.

[18] K. Pahlavan and A. H. Levesque, *Wireless Information Networks*, John Wiley & Sons, New York, 1995.

[19] P. Petrus, J. H. Reed, and T. S. Rappaport, "Geometrical-Based Statistical Macro cell Channel Model for Mobile environments," *IEEE Trans. Commun.*, vol. 50, no. 3, March 2002.

[20] Y. Chen and V. K. Dubey, "A Generic Channel Model in Multi-cluster environments," in *VTC*, Apr. 2003, vol. 1, pp. 217–221.

[21] M. Steinbauer, A. F. Molisch, and E. Bonek, "The Double-Directional Radio Channel," *IEEE Antennas Propag. Mag.*, vol. 43, pp. 51–63, Aug. 2001.

[22] A. F. Molisch, "A Generic Model For MIMO Wireless Propagation Channels in Macro- and Microcells," *IEEE Trans. Signal Process.*, vol. 52, no. 1, Jan. 2004.

[23] A. F. Molish, H. Asplund, R. Heddergott, M. Steinbauer, and T. Zwick, "The COST 259 Directional Channel Model-Part I: Overview and Methodology," *IEEE Trans. Wireless Commun.*, vol. 5, no. 12, pp. 3421–3433, 2006.

[24] J. Meinilä, P. Kyösti, L. Hentilä, T. Jäms"a, E. Suikkanen, E. Kunnari, and M. Narandžić, "D5.3: WINNER+ Final Channel Models," June 2010.

[25] J. L. Burbank, J. Andrusenko, J. S. Everett, and W. T. M. Kasch, *Wireless Networking Understanding Internetworking Challenges*, IEEE Press, Piscataway, New Jersey, 2013.

[26] 3GPP TR 36.814 V9.00 3rd, *Further advancements for E-UTRA physical layer aspects*, Mar. 2010.

[27] 3GPP TR 37.840 V12.00, *Study of Radio Frequency (RF) and Electromagnetic Compatibility (EMC) requirements for Active Antenna Array System (AAS) base station*, Mar. 2013.

[28] R1-xxxxxx, "Polarization Model for 3D Channel, Orange," *Submitted offline, http://www.flexible-radio.com/sites/default/files/attachments-186/Polarization%20Model%20For%203D%20Channel.pdf*, Aug. 2013.

[29] R1-136021, "TP for Mechanical Tilt," *NSN, Nokia, 3GPP RAN WG1 Meeting #75*, Nov. 2011.

[30] R1-135312, "Field pattern model of polarized antennas," *Qualcomm, 3GPP RAN WG1 Meeting #75*, Nov. 2011.

[31] R1-135708, "Text Proposal on Mechanical and Electrical Antenna Tilting," *Fraunhofer IIS, 3GPP RAN WG1 Meeting #75*, Nov. 2011.

[32] R1-134980, *Study on 3D channel model for LTE (Release 12)*, Sept. 2013.

[33] R1-133528, "On Optional High Rise Scenario," *3GPP TSG-RAN WG1 Meeting #74*, Aug. 2013.

[34] F. Ikegami, S. Yoshida, T. Takeuchi, and M. Umehira, "Propagation Factors Controlling Mean Field Strengthb on Urban Streets," *IEEE Trans. Antennas Propag.*, vol. 32, pp. 822–829, 1984.

[35] R1-135948, "Remaining details of fast-fading for 3D-UMa and 3D-UMa," Nov. 2013.

[36] R1-136000, "WF on RSRP calculation formula," *3GPP TSG RAN WG1 Meeting #75*, Nov. 2013.

[37] R1-134069, "Simulation assumptions for calibration and baseline performance evaluation," *Huawei, HiSilicon, 3GPP TSG RAN WG1 Meeting #75*, Nov. 2013.